Important electron-electron interaction and spin-orbit effects in thin copper films

Yael Fehr, Sharon May-tal, and Ralph Rosenbaum
School of Physics and Astronomy, Raymond and Beverly Sackler Faculty of Exact Sciences, Tel Aviv University, Ramat Aviv, Tel Aviv 69978, Israel
(Received 31 December 1985)

Resistance and magnetoresistance measurements on thin two-dimensional Cu films have been performed as a function of magnetic field and temperature. Electron-electron interaction effects were observed to make an important contribution to the logarithmic temperature rise of the resistance at low temperatures; the three-dimensional electron-screening integral factor F was found to take on a value of $F=0.54+0.05$ from the high-magnetic-field resistance data. The spin-orbit scattering also played a significant role in the negative magnetoconductance and became a factor of 30 stronger as the thickness of the Cu films was reduced from 140 to 34 Å. A simple analysis employing the interaction and weak-localization theories was used; predicted values of the resistances generally agreed with the experimental data. Values for the spin-orbit scattering time and inelastic scattering time are in general agreement with several recent theories. Analysis of the data from very thin percolating "semicontinuous" films was also performed successfully.

I. INTRODUCTION

Recent theories have predicted an anomalous logarithmic temperature dependence of the metallic resistance in thin two-dimensional (2D) films at low temperatures. There are two mechanisms that might be responsible for this behavior: a weak localization of noninteracting electrons[1,2] and an alternative explanation based on the Coulomb electron-electron interactions.[3-5] As Altshuler *et al.* have shown theoretically, the effects of these two mechanisms can be distinguished experimentally by measuring the resistance in a large constant magnetic field which "quenches" the weak-localization contribution.[4,6] Komnik *et al.* clearly demonstrated the separation of the weak-localization and electron-electron interaction effects in bismuth films.[7]

Localization studies in thin 2D Cu films have been conducted by at least three different groups in order to extract information on the electron scattering mechanisms in Cu. These mechanisms include the inelastic scattering time $\tau_i(T)$, the spin-orbit scattering time τ_{so}, and the magnetic scattering time τ_s.

A clear demonstration of the presence of electron-electron interactions in thin 2D Cu films has yet to be published; however, speculations, suggestions, and some experimental data on one-dimensional (1D) Cu wires have been published that suggest that interaction effects do exist in Cu. This paper presents new data on Cu films which clearly illustrate the importance of electron-electron interactions in Cu films. In Sec. II we review earlier measurements on Cu films, and in Sec. III, we discuss the theoretical results of the weak-localization and interaction theories and the percolation effects upon weak localization. Section IV covers the topic of film preparation techniques, which was crucial in detecting the spin-orbit contribution to the magnetoresistance data, Sec. V presents the experimental results and data fitting, and Sec. VI concludes with a comparison between measured and theoretical scattering times.

II. HISTORICAL BACKGROUND

Van den Dries *et al.* carried out the first measurements on thin Cu films.[8] They observed a logarithmic temperature increase of the resistance at low temperature, a positive magnetoconductance (negative magnetoresistance) at high magnetic fields, and a spin-orbit contribution which increased as the thickness of their Cu films was decreased; they credited these effects to weak localization. No detailed analysis of the data was made, and hence no values for the scattering times are available. Van den Dries *et al.* speculated theoretically that the electron-electron interaction effects could contribute as much as 25% to the observed logarithmic temperature increase of the resistance. They left this point to be verified in future experiments. They predicted that the electron screening parameter F would have a value of 0.6. We also note that their films were covered with photoresist to prevent oxidation. Our own observations indicate that photoresist causes anomalous resistance behavior at low temperatures. Thus, we are suspicious of any data in which Cu comes in contact with photoresist.

Gershenson *et al.* immediately followed up with some extensive magnetoconductance (MC) measurements on Cu films.[9] Their results for the inelastic scattering time and spin-orbit scattering time are in close agreement with our findings in this paper; their times are consistently a factor of 3 larger (hence, a factor of 3 weaker) compared to our values. Interestingly, they initially measured the resistance of an uncoated Cu film in zero magnetic field and then in a magnetic field of 0.3 T and observed a small decrease of the resistance in the magnetic field. Gershenson and Gubankov attributed this behavior to the existence of electron-electron interactions in Cu. Unfortunately, Gershenson *et al.* later proceeded to coat their films with photoresist. They then reported no change in the resistance even in moderately high magnetic fields of 1 T. They incorrectly concluded that the electron screening parameter F in Cu films is very small and they set $F=0$.

Interestingly, their choice of F fixed the prefactor parameter of their $\ln T$ interaction contribution to the value of one, namely, $g_{\rm eff}=(1-F)=1$. We find experimentally in this paper that $g_{\rm eff}\simeq 1$. It is, perhaps, fortuitous that these two results for $g_{\rm eff}$ agree so closely.

We have measured the properties of thin Cu films.[10] Our earliest papers too have been plagued with incorrect conclusions. In our first measurements,[10(a),10(b)] we failed to realize the importance of electron-electron interactions; hence, we failed to measure the resistance of the films in large perpendicular magnetic fields. In a later paper,[10(d)] we made measurements on Cu films in parallel magnetic fields. In this work we clearly saw signatures of the electron-electron interactions and concluded that the screening constant F took on a small magnitude of $F\cong 0.2$. Unfortunately, these Cu films were contaminated with magnetic impurities which were unintentionally introduced when we sliced up the high-purity copper wire with steel scissors. Some of these Cu films also had thin coatings of Pb to enhance the spin-orbit scattering. Hence, an "accurate" observation of the electron-electron interaction was not possible in this paper.

Lastly, White *et al.* measured the low-temperature resistance rise in 1D ultrathin wires.[11] Their best measurements are on Cu wires in which the data can be explained if only interaction effects are present. White *et al.* concluded that the value of the screening constant F is $F\cong 0.3\pm 0.2$.

In conclusion, the experimental results on 2D Cu films suggested values for the electron screening constant F which were considerably smaller than the predicted value. We were motivated to restudy the Cu films and to resolve this question.

Interaction effects are not the only mechanism to have a major influence on the zero-field resistance at low temperatures. Within the weak-localization framework, the spin-orbit scattering time $\tau_{\rm so}$ plays an important role in the zero-field resistance. This point was pursued by Gershenson *et al.*[9] but was missed by Van den Dries *et al.* and ourselves in the early studies.[8,10] The spin-orbit scattering time in Cu is significant (on the order of 10^{-12} sec) according to the prediction of Meservey and Tedrow:[12]

$$\tau_{\rm so}=\tau_0\frac{1}{(\alpha Z)^4}\ , \tag{1}$$

where τ_0 is the elastic scattering time, Z is the atomic number ($Z_{\rm Cu}=29$), and α is the fine structure constant $\alpha=\frac{1}{137}$. Both Van den Dries *et al.* and ourselves have observed that the elastic time depends directly upon the film thickness d as[8,10]

$$\tau_0=d/v_F\ , \tag{2}$$

where v_F is the Fermi velocity (for Cu, $v_F=1.56\times 10^6$ m/sec). Note that the spin-orbit scattering time is temperature independent. The spin-orbit scattering time can be determined experimentally from the analysis of the negative magnetoconductance data at small magnetic fields.

According to the weak-localization theory, the slope per temperature decade S of the resistance in the logarithmic region depends upon the spin-orbit scattering time $\tau_{\rm so}$ and upon the inelastic scattering time $\tau_i(T)$ in a rather complicated way.[13] In the case of very strong spin-orbit scattering, "antilocalization" is predicted in which case the resistance decreases logarithmically with a slope per temperature decade of $(\frac{1}{2})(\ln 10)e^2/(2\pi^2\hbar)$.[14] In the absence of spin-orbit scattering, the resistance increases logarithmically with a slope of $p(\ln 10)e^2/(2\pi^2\hbar)$; here, p is the exponent of the temperature dependence of the inelastic scattering time where $\tau_i(T)\propto T^{-p}$. Numerous authors have predicted different values for p ranging from 1 to 4; we will discuss some of the theoretical predictions later. The magnitude and temperature dependence of the inelastic scattering time $\tau_i(T)$ can be determined experimentally by analyzing the high-field magnetoconductance data at different temperatures. Thus, part of the zero-field temperature dependence of the resistance is determined by a delicate interplay between the spin-orbit and inelastic scattering times. This dependence is illustrated in Fig. 1 for a 75-Å Cu film where we have used our zero-field resistance data from Ref. 10(a). Curve a, which coincides very well with the data, includes only the inelastic scattering time using the weak-localization formalism; here $p=2$ was used. When the spin-orbit time is introduced as predicted from Eqs. (1) and (2), one obtains the antilocalization curve b, which is in complete disagreement with the data. However, when the electron-electron interaction contribution is introduced, the results are in reasonable agreement with the data, at least in the higher-temperature interval between 8 to 15 K. The electron-electron interaction term was calculated using (a) the value of Van den Dries *et al.* (Ref. 8) of $F=0.6$ (Ref. 8) and the $\ln T$ prefactor $g_{\rm eff}=2-2F=0.8$. From Fig. 1 we conclude that one cannot extract much information from the zero-field resistance curve since the logarithmic divergence of R at low temperatures is due probably both to weak-localization and electron-electron interactions. The spin-orbit scattering is known to be depressed by the pres-

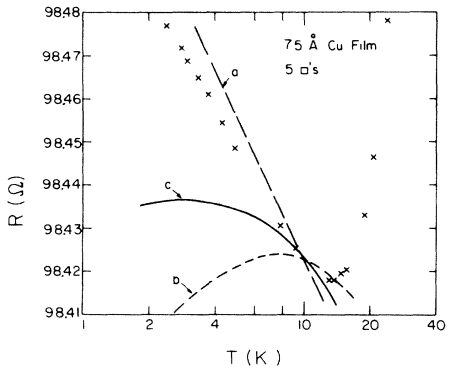

FIG. 1. Predictions of resistance versus temperature for different scattering processes in a 75-Å Cu film: curve a—WL theory with inelastic scattering only, curve b—WL theory with inelastic and spin-orbit scattering, curve c—includes both the electron interaction theory with $g_{\rm eff}=0.8$ and the WL theory with inelastic and spin-orbit scattering. The ×'s are data taken from an earlier paper for a 75-Å Cu film having 15 Ω/□ (Ref. 10).

ence of magnetic impurities in the films.[15] We have tried carefully to eliminate magnetic impurities during the preparation of the films in order to obtain new information on τ_{so}.

Lastly, Van den Dries *et al* have observed that very thin Cu films become "semicontinuous" for thickness less than 65 Å.[8] We have studied Cu films near the percolation threshold and present new data on these semicontinuous films.

III. THEORETICAL BACKGROUND

A. Weak-localization theory using perpendicular magnetic fields

For thin 2D films exhibiting weak localization, the general case of perpendicular magnetoconductance was derived by Hikami *et al.*,[13] and further studied by Maekawa and Fukuyama.[16] It is convenient to express the parameters of the theory in terms of "characteristic" fields, since in many cases these parameters can be obtained directly by careful extrapolation of the magnetoconductance data.[10] Bergmann introduced this concept of a characteristic magnetic field, and he was one of the first to extract spin-orbit and magnetic scattering times from this theory.[14,15] The effective field B_x is related to the scattering time τ_x through the relation

$$B_x=\hbar/4eD\tau_x \ , \tag{3}$$

where $D=v_F^2\tau_0/3$ is the three-dimensional diffusion constant and τ_0 is the elastic scattering time. For the case of Cu and using Eq. (2), we find that $D=v_F d/3$. For our Cu films, the elastic time is typically 10^{-14} to 10^{-15} sec corresponding to effective fields B_0 of 4 to 24 T.

According to the weak-localization (WL) theory of Hikami *et al.*,[13] the conductance per film square in a perpendicular magnetic field B, $\sigma_{\square,\mathrm{WL}}(B,T)$ takes on the following temperature dependence:

$$\begin{aligned}\sigma_{\square,\mathrm{WL}}(B,T)&=\sigma_0+\frac{e^2}{2\pi^2\hbar}f_1(B,T)\\&=\sigma_0+\frac{e^2}{2\pi^2\hbar}\left[\tfrac{3}{2}\psi\left(\frac{1}{2}+\frac{B_2}{B}\right)-\psi\left(\frac{1}{2}+\frac{B_1}{B}\right)-\tfrac{1}{2}\psi\left(\frac{1}{2}+\frac{B_3}{B}\right)\right] ,\end{aligned} \tag{4}$$

where ψ is the digamma function and where

$$\begin{aligned}B_1&=B_0+B_{so}+B_s \ ,\\B_2&=B_i(T)+4B_{so}/3+2B_s/3 \ ,\\B_3&=B_i(T)+2B_s \ .\end{aligned} \tag{5}$$

In Eq. (5), B_{so} is the characteristic spin-orbit field, B_s is the characteristic magnetic impurity field, $B_i(T)$ is the characteristic inelastic scattering field, and B is the applied perpendicular field. $B_i(T)$ had been observed previously for "clean" Cu films and typically assumed a value of $0.8\times10^{-4}T^2$ T above 10 K. The Cu films are extremely sensitive to magnetic impurities, and B_s can assume values from 0 to 0.003 T depending on the purity of the Cu material and the technique used to cut up the starting material for evaporation. Small changes in B_s will dramatically influence the sign of the perpendicular magnetoconductance in small fields.[15] For clean Cu films, B_{so} typically assumes a value of 0.004 T. σ_0 is an adjustable parameter chosen by fitting one of the reduced resistance data points to Eq. (4).

Using the definition of the magnetoconductance $\Delta\sigma_\square(B,T)$,

$$\begin{aligned}\Delta\sigma_\square(B,T)&=\sigma_\square(B,T)-\sigma_\square(0,T)\\&=1/R_\square(B,T)-1/R_\square(0,T) \ ,\end{aligned} \tag{6}$$

the expression for the perpendicular magnetoconductance becomes [Eqs. (4) and (6)]

$$\begin{aligned}\Delta\sigma_{\square,\mathrm{WL}}(B,T)&=\frac{e^2}{2\pi^2\hbar}f_2(B,T)\\&=\frac{e^2}{2\pi^2\hbar}\left[\tfrac{3}{2}\psi\left(\frac{1}{2}+\frac{B_2}{B}\right)-\psi\left(\frac{1}{2}+\frac{B_1}{B}\right)-\tfrac{1}{2}\psi\left(\frac{1}{2}+\frac{B_3}{B}\right)-\ln\left(\frac{B_2^{3/2}}{B_1B_3^{1/2}}\right)\right] .\end{aligned} \tag{7}$$

Although Eq. (7) is often simplified for small values of B and B_x, the full expression was used, since in these measurements the condition $B>B_0$ existed for some of the data points, while the condition $B<B_{so}$ existed for other data points. It should be noted that for the highest field employed of 7.5 T, the films are no longer strictly 2D since $l_B=(\hbar/2eB)^{1/2}=d$. The WL expressions are valid only if the conditions $d<(D\tau_i)^{1/2}$ and $d<l_B$ are satisfied.

B. Electron-electron interaction theories

Altshuler *et al.* calculated a different mechanism to the resistance at low temperatures caused by the mutual Coulomb interactions in the presence of scattering by normal impurities;[3] they considered orbital effects only. They obtained a zero-field correction for the conductance of a thin film, similar to the case of weak localization:

$$\sigma_{\square,e\text{-}e}(T)=\sigma_0-\frac{e^2}{2\pi^2\hbar}(1-F)\ln(\tau_T/\tau_0) \ , \tag{8}$$

where F is the three-dimensional screening integral factor and $\tau_T=\hbar/2\pi k_BT$ is a characteristic thermal diffusion time. Fukuyama derived a slightly different expression for the case of weak spin-orbit interaction:[17]

$$\sigma_{\square,e\text{-}e}(T)=\sigma_0-g\frac{e^2}{2\pi^2\hbar}\ln(\hbar/4\pi k_BT\tau_0) \ , \tag{9}$$

where g is defined in terms of effective interaction constants

$$g=g_1+g_2-2(g_3+g_4) \ . \tag{10}$$

Here, g_1 and g_2 are the sum of the exchange-type correc-

tions with particle-hole and particle-particle diffusion processes and g_3 and g_4 are some of the corresponding Hartree-type corrections. When the interaction is of dynamically screened Coulomb type with $g_1=1$ and $g_2=g_3=g_4=F/2$, Eqs. (10) and (9) change simply to

$$\sigma_{\square,e\text{-}e}(T)=\sigma_0-\frac{e^2}{2\pi^2\hbar}(1-3F/2)\ln(\hbar/4\pi k_B T\tau_0)\ . \quad (11)$$

We note that Eqs. (8) and (11) differ by a prefactor of $F/2$ and differ also in the characteristic diffusion time τ_T by a factor of 2. Values of τ_T vary between $\hbar/k_BT$ and $\hbar/4\pi k_BT$ in the literature. Its exact value becomes important when we calculate the criterion for two dimensionality, namely, $d<(D\tau_T)^{1/2}$. We calculate that the highest temperature at which this theory is still valid ranges from 40 to 400 K, depending upon which factor is used. Additional theoretical work is needed to clarify these differences. In addition, Fukuyama included a second term in Eq. (9) which he denoted as[17]

$$(e^2/2\pi^2\hbar)(g_2-2g_4)\phi(h,\gamma)\ .$$

We have neglected this term, as our data do not require its contribution. The reader is referred to Ref. 17 for further details.

Lee and Ramakrishnan considered spin effects in the interaction theory.[18] They studied the magnetoconductance due to the splitting of the spin-up and spin-down bands in a magnetic field; their results lead to a positive contribution to the magnetoresistance (negative MC). They also give an expression for the conductance [Eq. (2.6a) in Ref. 18] which we interpret as a contribution resulting from spin splitting only:

$$\sigma_{\square,e\text{-}e}(T,B)=\sigma_0-\frac{e^2}{2\pi^2\hbar}(1-F/2)\ln(\tau_T/\tau_0)-\frac{e^2}{2\pi^2\hbar}\frac{F}{2}g_2(h)\ . \quad (12)$$

Again, the third term of Eq. (12) involving $g_2(h)$ is very small in our case of Cu and we have neglected this term in the analysis of the resistance and MC data.

We have combined the orbital results of Eq. (11) with the spin results of Eq. (12) to obtain the electron-electron interaction expression which we will use to analyze the resistance data:

$$\sigma_{\square,e\text{-}e}(T)=\sigma_0-\frac{e^2}{2\pi^2\hbar}(2-2F)\ln(\hbar/4\pi k_B T\tau_0)\ . \quad (13)$$

Equation (13) differs from the results of Altshuler *et al.* only by a prefactor of 2. This factor of 2 was crucial to the successful interpretation of our data. Note that for either expression, there is the common term $(1-F)$ in the prefactor. For very weak electron-electron interactions, we demand that this term $(1-F)$ be zero, thus implying that $F\cong 1$. In the opposite case of strong electron-electron interactions, we want the prefactor to take on the maximum value of either 1 or 2; in this case $F\cong 0$.

The final expression for the conductance of the film consists of the WL contribution, Eq. (4), and the electron-electron interaction contribution, either Eq. (8) or Eq. (13),

$$\sigma_{\square}(B,T)=\sigma_0+\frac{e^2}{2\pi^2\hbar}f_1(B,T)-\frac{e^2}{2\pi^2\hbar}g_{\rm eff}\ln(\hbar/4\pi k_B T\tau_0)\ , \quad (14)$$

where $g_{\rm eff}=(2-2F)$ in one case and $g_{\rm eff}=(1-F)$ in the second case.

The screening constant F depends upon the three-dimensional screening length l_s in a complicated matter. Recall that the screening length l_s appears in the screened Coulomb potential, $\phi(r)=Ze^2/(4\pi\epsilon_0 r)e^{-r/l_s}$. In very low electron-density materials where l_s is large, the screened Coulomb potential reduces to the bare-range Coulomb potential; in this case, strong electron-electron interactions would be anticipated leading to a large value of the prefactor term $(1-F)$ and a small value for F. For the other case of a high electron-density material where l_s is small, the screened potential rapidly decays with distance r, and electron-electron interactions should be weak, leading to a small prefactor value for $(1-F)$ and a value of F close to unity. For this case, the screening is complete. We have chosen to use the definition of l_s as defined by Ashcroft and Mermin,[19]

$$l_s=(\pi a_0/4k_F)^{1/2}\ , \quad (15)$$

where a_0 is the Bohr radius ($a_0=0.53$ Å) and k_F for Cu is $k_F=1.36\times10^8$ cm^{-1}. We calculate $l_s=0.55$ Å for Cu. We use the approximation made by P. A. Lee for the scattering matrix element over the Fermi sphere that[8]

$$F=(1/2k_F l_s)^2\ln[1+(2k_F l_s)^2]\ . \quad (16)$$

We find that the screening constant takes on a value of $F=0.53$ as compared to the calculated value of Van den Dries *et al.* of $F=0.6$. We anticipate that the prefactor of electron-electron contribution, $g_{\rm eff}$, as given by $2(1-F)$ and $(1-F)$ will take on the value of 0.94 or 0.47. Thus, the electron-electron interactions are predicted to be important in Cu.

C. Percolation effects on weak localization

Van den Dries *et al.* first observed that their very thinnest Cu films exhibited semicontinuous, percolating properties.[8] They had observed that for their continuous Cu films, the resistance per square $R_\square$ followed a d^{-2} dependence on the film thickness d. We reconfirmed these results observing that[10]

$$R_\square=m^*v_F/ne^2d^2=8.7\times10^4/d^2(\Omega/\square)\ , \quad (17)$$

where d is in units of Å. For films having thicknesses less than about 65 Å, their measured $R_\square$ was much greater than those predicted by Eq. (17). Van den Dries *et al.* speculated that the thinner films became discontinuous through the appearance of cracks in the films. We have taken transmission electron microscope (TEM) pictures of two Cu films deposited on thin 300-Å carbon supporting substrates; one film was a fresh 60-Å continuous film, while the second film was allowed to oxidize until it became nonconducting. The results are shown in Fig. 2. For the continuous film, there are indications of

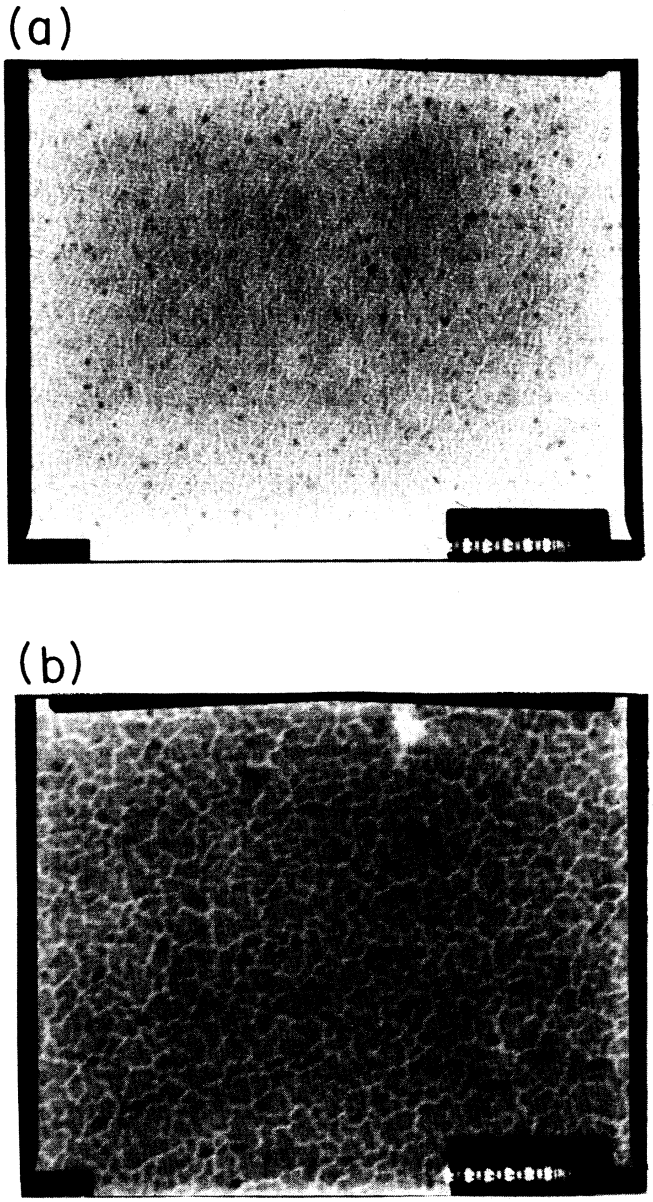

FIG. 2. TEM pictures of a 60-Å Cu film: (a) unoxidized semicontinuous film showing the weak appearance of cracks, and (b) oxidized noncontinuous film showing isolated 75-Å islands separated by cracks permeating throughout the entire film.

the development of thin cracks [Fig. 2(a)]. The noncontinuous film has cracks permeating throughout the film [Fig. 2(b)]. The width of the cracks is very small, on the order of 10 to 20 Å. The typical size of the isolated islands is on the order of 75 to 100 Å. We believe that similar behavior occurs on the glass substrates used in the actual measurements.

The development of cracks and the existence of isolated nonconducting islands throughout the film have a direct bearing upon the magnitude of the magnetoconductance of the film. Van den Dries *et al.* had made the important observation that the MC values of their semicontinuous films were smaller by a factor of 4 compared to the MC values of their continuous films. This result can be explained using the following rough model. In this model, one discards all of the nonconducting islands and channels and "combines" all of the remaining conducting, narrow, channels into a new hypothetical film having an "effective" width that is smaller than the original film width. This imaginary film will have a larger number of squares, $N_{\square}^{\text{theor}}$, than the number of squares, $N_{\square}^{\text{expt}}$ present in the continuous film since the number of squares is determined by the ratio of the constant film length to its effective width. Note that the number of squares, $N_{\square}$, directly determines the magnitude of the MC data, since from Eq. (6),

$$\Delta\sigma_{\square}=1/R_{\square}(B)-1/R_{\square}(B=0)=N_{\square}/R(B)-N_{\square}/R(0)\ .$$

The experimentalist has one of two choices for his semicontinuous films. Either he must scale up his experimental MC data by a prefactor which is generally not known initially, or he must scale down the predictions of Eq. (7), using a prefactor $N_{\square}^{\text{expt}}/N_{\square}^{\text{theor}}$, to the MC data that had previously been normalized using the number of squares appearing in the continuous films, namely, $N_{\square}^{\text{expt}}$. For our continuous films, $N_{\square}^{\text{expt}}=10\pm0.5$ squares.

Recently, Palevski and Deutscher have proposed an expression for the scaling down prefactor, which they denote as $R(\langle l_i\rangle)/R_{\square}$.[20] They find that

$$R(\langle l_i\rangle)/R_{\square}=\frac{r_{\square}}{R_{\square}}\left[\frac{l_i}{\omega}\right]^{\mu/\nu}\ , \tag{18}$$

where $R_{\square}$ is the actual film resistance normalized to the number of squares $N_{\square}^{\text{expt}}$ appearing in the continuous films, $r_{\square}$ is the hypothetical resistance per square for a film of the same thickness if it were continuous [given by Eq. (17)], l_i is the inelastic scattering length given by $l_i=(D\tau_i)^{1/2}$, w is the width of a typical conducting channel in the semicontinuous film which can be obtained from TEM pictures, and μ and ν are critical indices of the conductivity and of the percolation correlation length ξ_p as defined by $\sigma\propto|p-p_c|^{\mu}$ and $\xi_p\propto|p-p_c|^{-\nu}$. The percolation correlation length, or the connectivity length ξ_p, is a measure of the size of a typical nonconducting region in the film. Palevski and Deutscher experimentally observed that $\mu/\nu=0.95$.[21] We evaluate Eq. (18) for our 34-Å film. Experimentally, we measure $R=45\,000\ \Omega$, and using 10 squares for the continuous film, $R_{\square}=4500\ \Omega/\square$. From Eq. (17) we predict that $r_{\square}=75\ \Omega/\square$ for a continuous 34-Å film. From the TEM picture of Fig. 2(b), the width of the conducting channel w is typically the width of one of the isolated islands, namely, about 75 Å. At 10 K, τ_i is typically 6×10^{-13} sec yielding $l_i=330$ Å.[10] We find that $R(\langle l_i\rangle)/R_{\square}=0.07$. The computer fit to the resistance and MC data yielded $N_{\square}^{\text{expt}}/N_{\square}^{\text{theor}}=10$ squares/65 squares$=0.15$, certainly in reasonable agreement with the Palevski and Deutscher value.

The fit to our 34- and 38-Å semicontinuous film data was performed as follows. To simplify the analysis we have set $R(\langle l_i\rangle)/R_{\square}=N_{\square}^{\text{expt}}/N_{\square}^{\text{theor}}$ and we treat this prefactor as a temperature-independent parameter. The

scaled down version of Eq. (7), namely,

$$\Delta\sigma_{\square,\mathrm{WL}}=\frac{e^2}{2\pi^2\hbar}\frac{N_{\square}^{\mathrm{expt}}}{N_{\square}^{\mathrm{theor}}}f_2(B,t)\ , \tag{19}$$

with the three parameters, $N_{\square}^{\mathrm{expt}}/N_{\square}^{\mathrm{theor}}$, $B_i(T)$, and B_{so}, was fitted to the MC data (based upon $N_{\square}^{\mathrm{expt}}=10$ squares). Since the value of $N_{\square}^{\mathrm{theor}}$ is now known, the resistance data have been converted to the conductance per square using $\sigma_{\square}=1/R_{\square}=N_{\square}^{\mathrm{theor}}/R$. The conductance data at each magnetic field were compared to Eq. (14). Equation (14) has two adjustable parameters, g_{eff} and σ_0. We set $g_{\mathrm{eff}}=0.93$, to be discussed later; σ_0 was chosen such that the predicted conductance agreed with the experimental conductance at one temperature point. If this fit was unsatisfactory, the process was repeated with a new trial value of $N_{\square}^{\mathrm{expt}}/N_{\square}^{\mathrm{theor}}$. Our observations indicate that whenever an excellent fit to the MC data was achieved, then the fit to the resistance data was also good. Thus, this technique seems to yield reasonable and consistent results.

IV. SAMPLE PREPARATION AND EXPERIMENTAL TECHNIQUES

Sample preparation of the films was crucial since contamination of their surfaces greatly deteriorated the localization effects. Surface contaminants such as photoresist, frozen air, or fingerprints all produced anomalous behaviors in the resistivity.[10] The films were made by evaporating 99.999% pure Cu onto glass microscope slides held at room temperature. The vacuum during evaporation was 10^{-5} mm Hg. One source of Cu was high-purity wire from Materials Research Corporation which we broke up into small sections manually using plastic gloves; thus, magnetic impurities from a steel scissors or cutter were avoided. A second source of Cu was a slug sliced up using a diamond saw. As another precaution to obtain clean Cu films, we replaced the old tungsten evaporation boat with a new boat. A metal mask was used to define the film geometry; each film was 1 mm wide and 10 mm long. Immediately after the evaporation, leads were attached to the film using pressed In contacts. Each film was transferred to the cryostat as quickly as possible to avoid oxidation and the development of cracks throughout the film. The time lapse between evaporation and cool down was less than one-half hour.

All of the magnetoconductance and resistance measurements were made using a superconducting magnet. Since many of the measurements were taken above 4 K, the films were inserted into a vacuum can centered inside the superconducting magnet. The sample cell was heated yielding a quasi-equilibrium temperature; temperatures were recordered with a calibrated Ge thermometer located inside the cell. An experimental problem arose with the MC measurements from small temperature drifts during heating. This problem became serious above 20 K where some of the low-resistance films (films having thicknesses greater than 50 Å) had a strong temperature dependence arising from electron-phonon scattering (see Fig. 1, for example). In this region, the resistance rose sharply with temperature as $R\propto T^{3.5}$. Thus, it was crucial to define temperature stability for $R(B=0,\ T)$ in the MC measure-

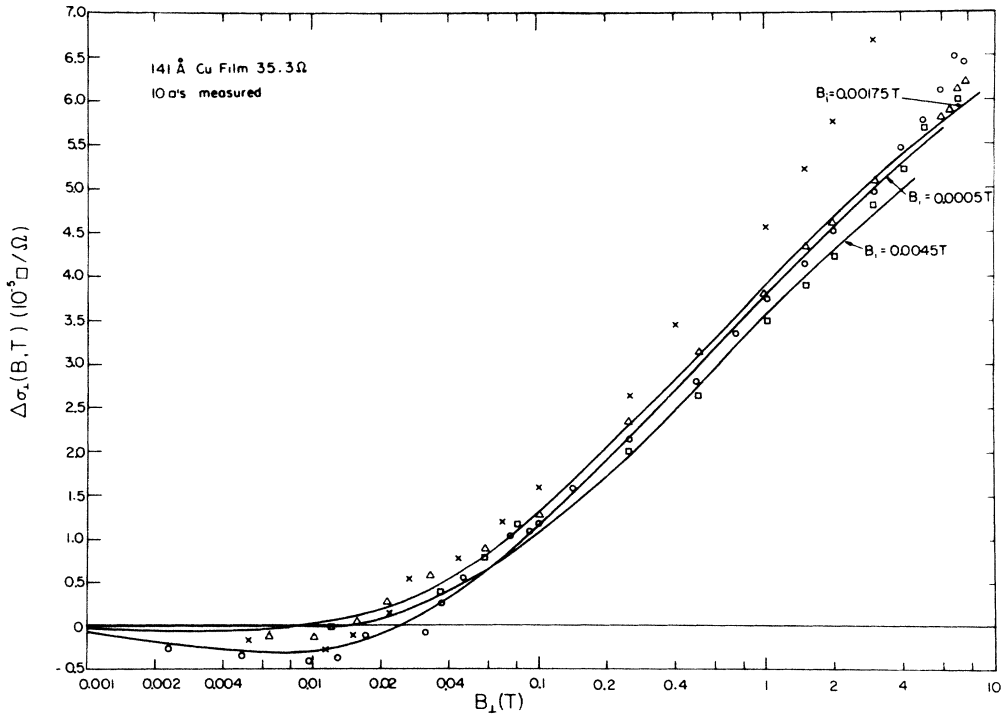

FIG. 3. Magnetoconductance (MC) versus magnetic field for a 141-Å Cu film having 3.53 Ω/□. A computer fit to the 1.9-K data was not possible. Note the negative MC values at small magnetic fields. The spin-orbit fitting parameter B_{so} was $B_{so}=0.0017$ T. Solid lines are fits using Eq. (7). × = 1.9 K, ○ = 4.2 K, △ = 8.7 K, and □ = 16.7 K.

ments, and continuous monitoring of the film resistance in zero field was required. This limited the accuracy of the MC data above 20 K to ±15%. At lower temperature, the MC data are accurate to ±5% and limited to our ability to determine the number of squares $N_{\square}^{\text{expt}}$ accurately in each film. Each film had 10±0.5 squares. At low temperatures the zero-field resistance can be maintained constant with temperature with great precision and the relative accuracy between MC points is better than ±2%. The resistance data is also accurate to ±3% and is limited to thermometry uncertainties.

Resistances were measured using the standard four-terminal voltage technique and employing the Hewlett Packard 3456A digital voltmeter. Currents of less than 10 μA were used to avoid Joule heating.

V. EXPERIMENTAL RESULTS AND DATA FITTING

For the "continuous" films having thicknesses of 141, 106, and 56 Å, the resistance and magnetoconductance results are presented in Figs. 3 through 8. Actually the 56-Å film is already slightly semicontinuous but we analyze its MC data as if the film were continuous and had 10 squares. At low perpendicular magnetic fields, the negative MC (positive magnetoresistance) in Figs. 3, 5, and 7 arises from the spin-orbit scattering; these negative MC magnitudes are the largest values we have observed, to the present, and indicate that these films are relatively free

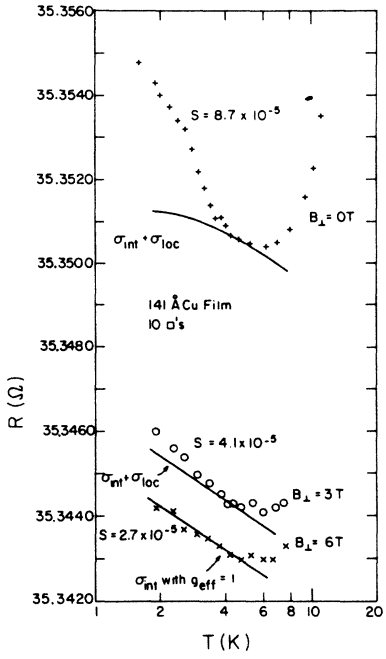

FIG. 4. Resistance of the 141-Å Cu film versus temperature at different applied perpendicular magnetic fields. S indicates the slopes per temperature decade in units of □/Ω. Solid lines are fits using Eq. (14). Note the strong antilocalization prediction in zero field and note the finite slope at $B=6$ T.

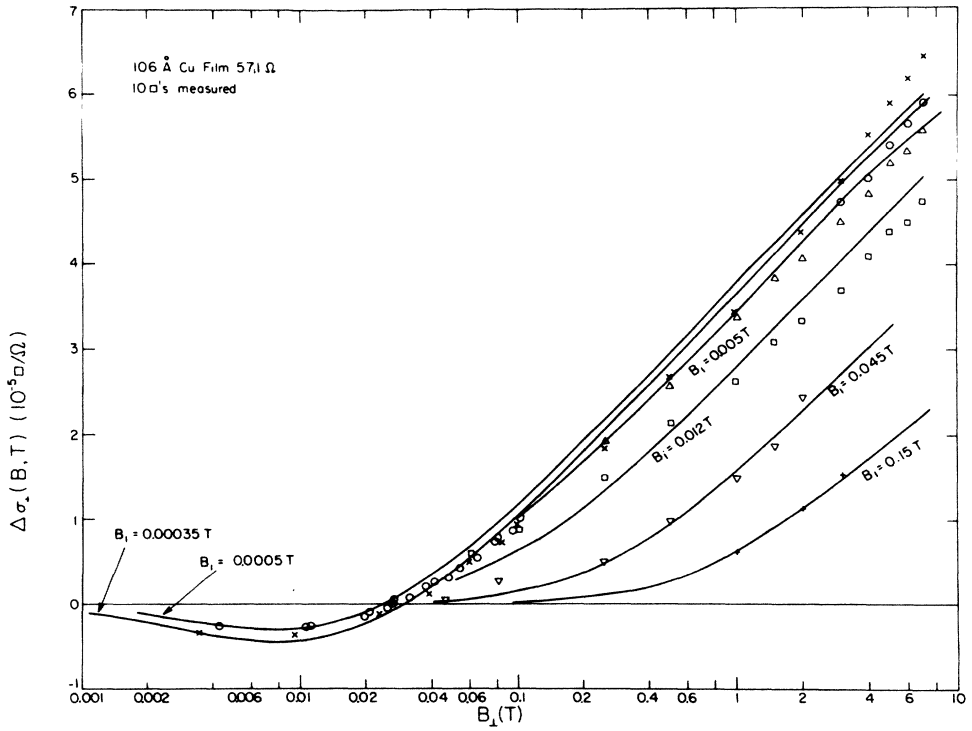

FIG. 5. MC versus magnetic field for a 106-Å Cu film having 5.71 Ω/□. Note the negative MC at small fields. $B_{so}=0.0017$ T. Solid lines are fits using Eq. (7). ×=2.0 K, ○=4.2 K, △=10 K, □=20 K, ▽=30.5 K, and + =53 K.

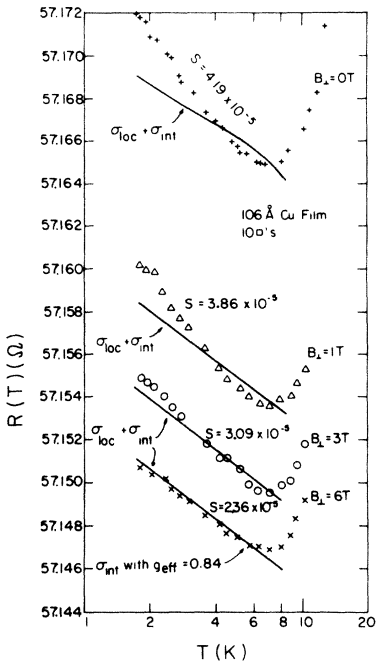

FIG. 6. Resistance of the 106-Å Cu film versus temperature at different applied fields. Solid lines are fits using Eq. (14). Note the finite slopes at $B=3$ and 6 T. The slopes have units of $\square/\Omega$.

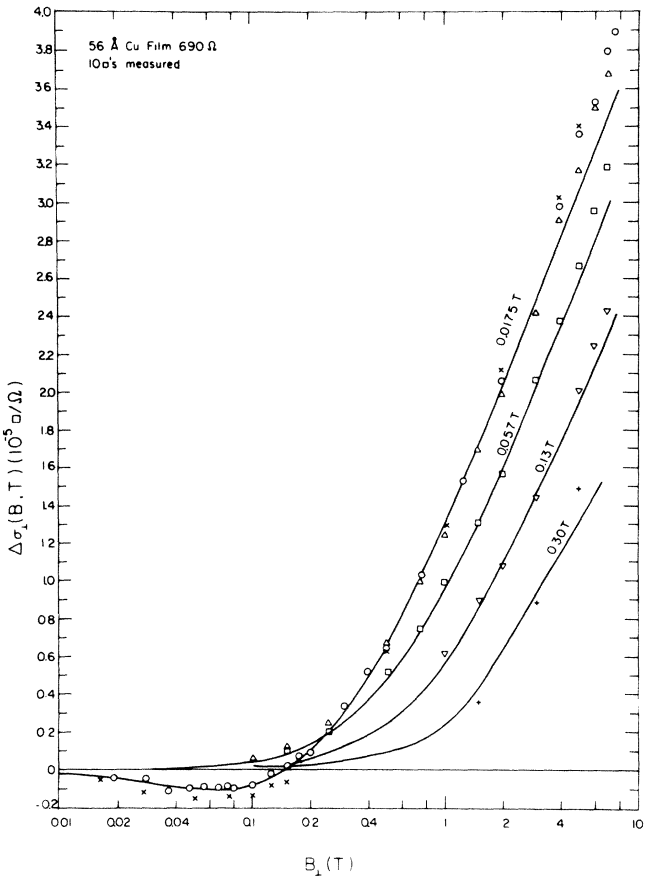

FIG. 7. MC versus magnetic field for a 56-Å Cu film having 69 $\Omega/\square$. Note the negative MC at moderate magnetic fields implying an increasing spin-orbit interaction. $B_{so}=0.0175$ T. Solid lines are fits using Eq. (7). $\times=2.0$ K, $\circ=4.2$ K, $\triangle=10$ K, $\square=20$ K, $\nabla=29$ K, and $+=50$ K.

from magnetic impurities. Hence, we have set the effective magnetic impurity field $B_s=0$. At higher fields, the MC exhibits the typical positive MC (negative magnetoresistance) characteristic of the weak-localization theory. The MC data were compared to Eq. (7) without using the interaction contributions suggested by Fukuyama and by Lee and Ramakrishnan.[17,18] Results for the spin-orbit scattering time and inelastic scattering time are shown in Figs. 13 and 14. These times were obtained from the characteristic magnetic fields, B_x, and Eq. (3) where $D=v_F d/3$. The characteristic fields come directly from fits of Eq. (7) to the MC data. Fits were possible to all the MC data with the exception of the 1.9-K data of the 141-Å film (Fig. 3) which showed anomalously high behavior at 1.9 K. Van den Dries *et al.* have suggested that this anomalous behavior arises from magnetic impurities and the Kondo effect in the thicker Cu films.[8] The predicted resistances from Eq. (14) are in good to poor agreement with the measured resistances (see Figs. 4, 6, and 8). The zero-field predictions all exhibit antilocalization behavior; part of the disagreement arises from our use of the inelastic magnetic field B_i having a T^2 dependence only in these fits, whereas the MC data indicated that at low temperatures the inelastic magnetic field B_i takes on a T^1 dependence. The other part of the disagreement appears to be an inherent problem in Eq. (14) at low magnetic fields. We simply have never been able to fit any of our resistance data of the thicker films in the low magnetic field region. This problem requires additional study.

Inspection of the high-field resistance data of Figs. 4, 6, and 8 reveals that slopes (per temperature decade) of the $\ln T$ dependence tend to the same finite value of about 2.6×10^{-5} $\square/\Omega$; we interpret this result as the electron-electron interaction contribution to the resistance. It would have been advantageous to extend the resistance measurements to fields greater than 7 T, but a stronger magnet was not available. The prefactor of the $\ln T$ term, $g_{\rm eff}$, takes on the mean value of $g_{\rm eff}\cong0.93$; if we accept the formalism of Eq. (13), where $g_{\rm eff}=2(1-F)$, then $F=0.54$ agrees with our screening-constant prediction of 0.53. If, however, one chooses the Altshuler *et al.* prefactor of $g_{\rm eff}=(1-F)$ of Eq. (8), then $F=0.08$, inferring that $l_s=2.6$ Å; this value of l_s is much greater than the predicted value of 0.55 Å from Eq. (15) and is in complete conflict with the theory.

The properties of the semicontinuous percolating films, or "inhomogeneous 2D" films, are shown in Figs. 9 through 12. The thicknesses of these two films are estimated as 34 and 38 Å. The spin-orbit interaction continues to increase with decreasing film thickness, as seen in Figs. 9 and 11. From Figs. 9 and 11, the MC data take on the same general form as seen in the continuous films

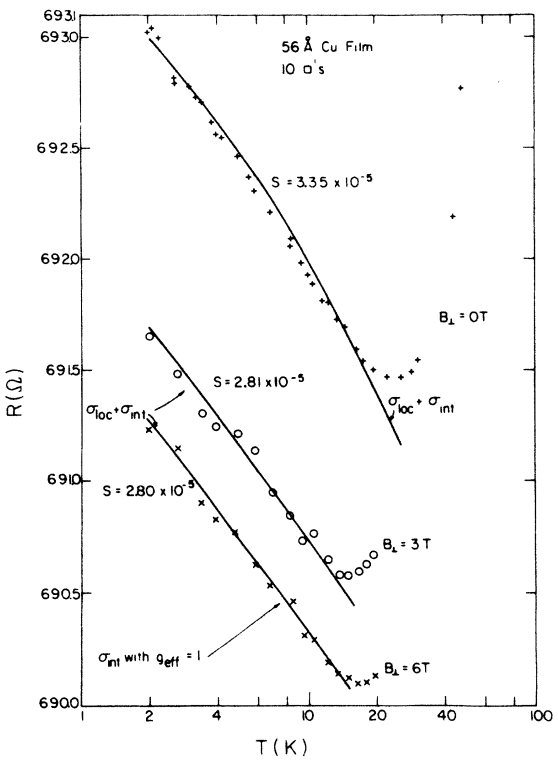

FIG. 8. Resistance of the 56-Å Cu film versus temperature at different applied fields. Solid lines are fits using Eq. (14). Note the finite slopes at $B=3$ and 6 T. The slopes have units of $\square/\Omega$.

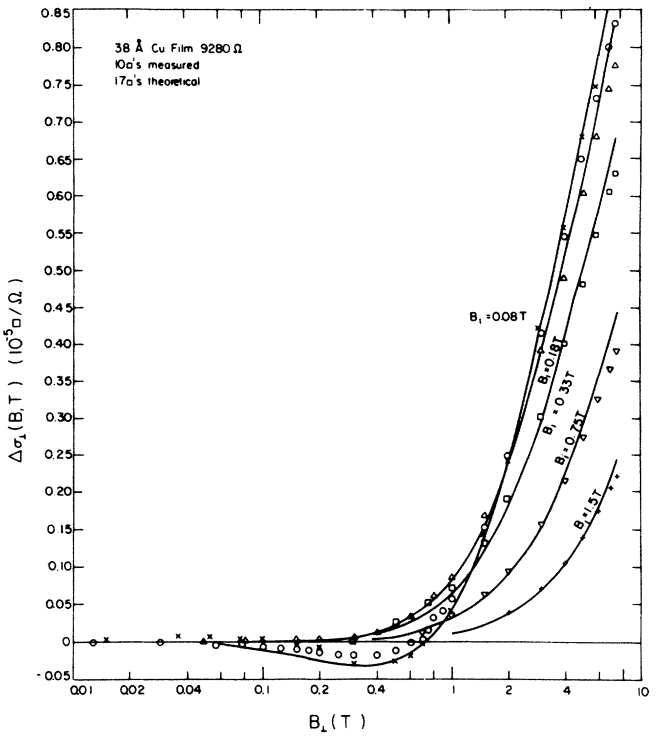

FIG. 9. MC versus magnetic field for a 38-Å semicontinuous Cu film having a "measured" 928 $\Omega/\square$. Note the small magnitude of the MC compared to the values of the MC in the continuous films of Figs. 3, 5, and 7. Also observe the strong spin-orbit effect present at $B=0.4$ T. $B_{so}=0.105$ T. Solid lines are fits using Eq. (19). $\times=1.95$ K, $\circ=4.2$ K, $\triangle=10.3$ K, $\square=18.2$ K, $\nabla=30.5$ K, and $+=43.5$ K. The fitting analysis suggests that this MC data should be scaled up by a factor of $\frac{17}{10}$.

except for one outstanding feature—the magnitudes of the MC data are almost a magnitude smaller than those of the continuous films. This observation is consistent with the findings of all of the earlier experimental works and fits well with the Palevski-Deutscher prediction in percolating films.[8,10,20]

The analysis of the MC and resistance data for these two semicontinuous films was more complicated than in the case of the continuous films. First, with reference to the continuous films, the analysis was straightforward. Fits to the MC data determined the values of $\tau_i(T)$ and τ_{so}. These times were then used to predict the experimental resistances. However, two parameters, σ_0 and $g_{\rm eff}$, appear in the conductance expression; $g_{\rm eff}$ was determined directly from the experimental slope of the high-field resistance data. The parameter σ_0 was chosen at each fixed magnetic field such that the predicted resistance curve would pass through one of the experimental measured points. These predicted resistance curves appear as the solid curves in Figs. 4, 6, and 8. But, in the semicontinuous films, two new problems arose. First, because the spin-orbit and inelastic times became much shorter (hence, much stronger), our largest magnetic field of 6 T did not entirely "quench" the WL contribution to the resistance; for the 34-Å film, the WL contributed 30% to the slope of the resistance data at 6 T. Since $g_{\rm eff}$ could not be determined directly from the 6-T data, we used the value $g_{\rm eff}$ observed in the continuous films, namely, $g_{\rm eff}=0.93$. The electron-electron interaction should not depend upon the film thickness nor upon the continuity of the film, since the screening length l_s is so much smaller than any other dimension. Moreover, there is now the additional parameter, the prefactor $R(\langle l_i\rangle)/R_\square$, to be determined. This prefactor cannot be uniquely determined by fitting only the MC data. A self-consistent calculation must be made since this prefactor determines the number of squares, $N_\square^{\rm theor}$, by which the predicted resistance values must be scaled up to the experimental values. After several iterations using different values for the prefactor $R(\langle l_i\rangle)/R_\square=N_\square^{\rm expt}/N_\square^{\rm theor}$, we were surprised to observe that the value that gave the best fit to the MC data also gave the best fit to the resistance data. In conclusion, we found that the theoretical number of squares for the 38- and 34-Å films were 17 and 65 squares, as compared to the measured value of 10 squares. Values of τ_{so} and $\tau_i(T)$ for these films are also shown in Figs. 13 and 14.

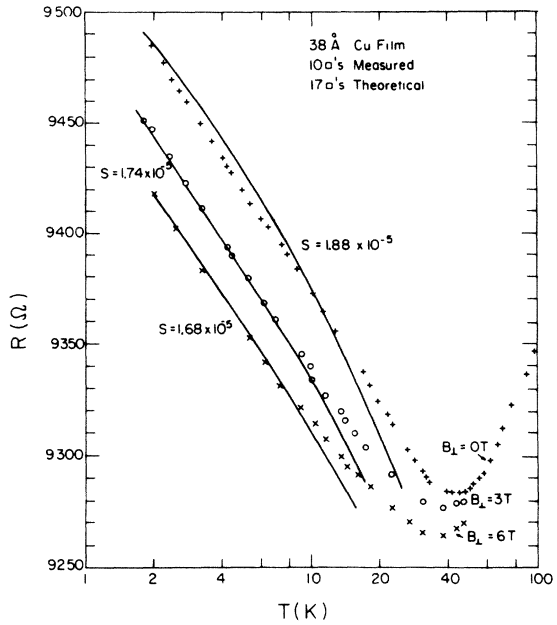

FIG. 10. Resistance of the 38-Å semicontinuous Cu film versus temperature at different applied fields. Solid lines are fits using Eq. (14) and using the fitting parameter $N_{\square}^{\text{theor}}=17$ squares instead of the measured $N_{\square}^{\text{expt}}=10$ squares owing to percolation effects in the semicontinuous film. The fitting analysis suggests that the slopes should be scaled up by the factor of $\frac{17}{10}$. Slopes have units of $\square/\Omega$.

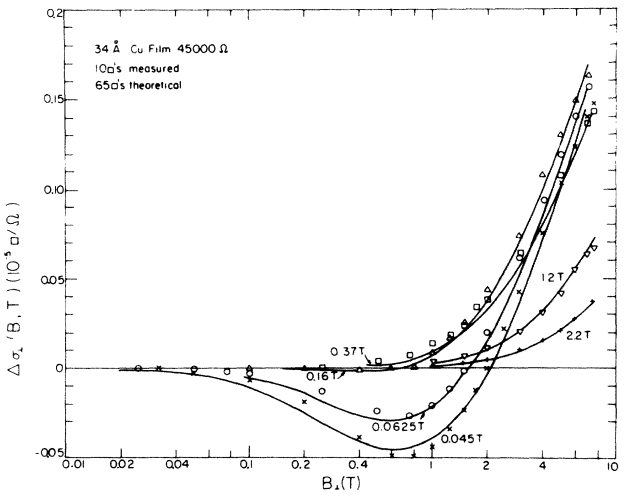

FIG. 11. MC versus magnetic field for a 34-Å semicontinuous Cu film having a measured 4500 $\Omega/\square$. Note the small magnitudes of the MC compared to the values of the MC in the continuous films of Figs. 3, 5, and 7. Also, observe the strong spin-orbit effect present at $B=0.7$ T. $B_{so}=0.15$ T. Solid lines are fits using Eq. (19). $\times=2.1$ K, $\circ=4.2$ K, $\triangle=10.5$ K, $\square=19$ K, $\triangledown=33$ K, and $+=49$ K. The fitting analysis suggests that this MC data should be scaled up by the factor of $\frac{65}{10}$.

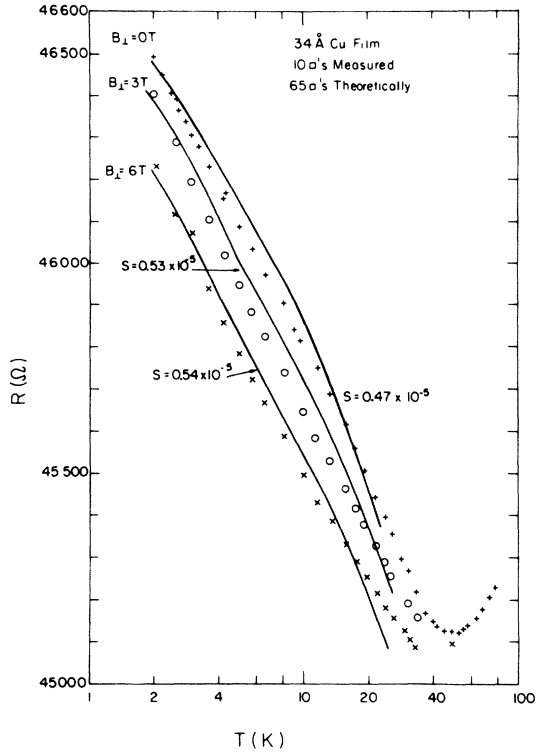

FIG. 12. Resistance of the 34-Å semicontinuous Cu film versus temperature at different applied fields. Solid lines are fits using Eq. (14) and using the fitting parameter $N_{\square}^{\text{theor}}=65$ squares instead of the measured $N_{\square}^{\text{expt}}=10$ squares arising from percolation effects in the semicontinuous film. The fitting analysis suggests that the slopes should be scaled up by a factor of $\frac{65}{10}$. Slopes have units of $\square/\Omega$.

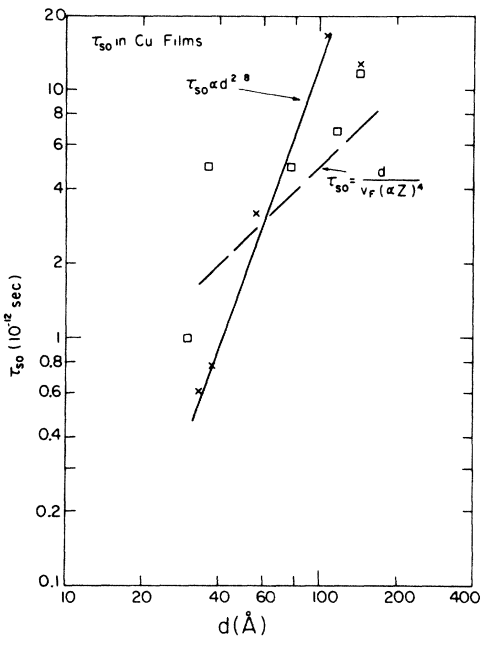

FIG. 13. Spin-orbit times versus film thickness. $\times=$data of this paper; $\square=$older data from Ref. 10. Dashed line is Eq. (1) from Ref. 12.

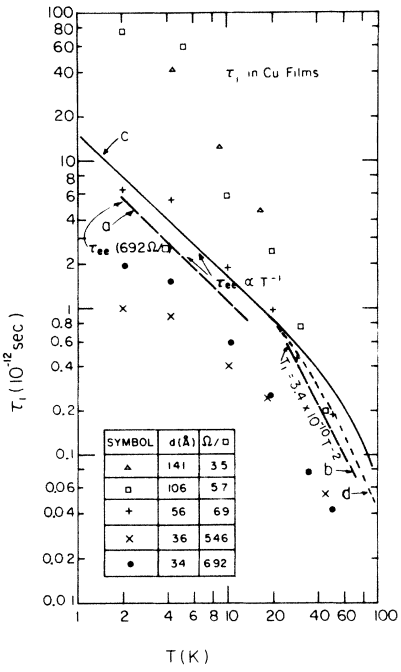

FIG. 14. Inelastic scattering times versus temperature for five different Cu films. Curve *a*—fit using Eq. (22) to $d=34$ Å, curve *b*—observed inelastic scattering time for a 75-Å Cu film from Ref. 10, curve *c*—fit using Eq. (21) and the inelastic scattering times given by Eqs. (22) and (30) for $l_0=d=56$ Å, and curve *d*—fitting conditions identical to curve *c* except that the electron-phonon scattering time of Eq. (30) was scaled smaller by a factor of 3. The values of the resistances per square appearing in the table are based upon $N_{\square}^{\text{theor}}$, not $N_{\square}^{\text{expt}}$.

VI. DISCUSSION

Fits of the weak-localization theory to the MC data were generally successful using the two adjustable parameters, τ_{so} and $\tau_i(T)$; values for these two scattering times agree within a factor of 3 with our earlier findings.[10]

The spin-orbit time has a considerably stronger dependence upon the film thickness d than predicted by Meservey and Tedrow [Eq. (1)], as can be seen in Fig. 13 with $\tau_{so} \propto d^3$. We suggest the existence of another spin-orbit scattering mechanism at the surface of the cracks, such that

$$\tau_{so}^{-1}=\tau_{so,\text{int}}^{-1}+\tau_{so,\text{cracks}}^{-1} , \tag{20}$$

where $\tau_{so,\text{int}}$ is given by Eq. (1) and $\tau_{so,\text{cracks}}$ is the spin-orbit scattering time arising from the interface. Theoretical work on this mechanism is required.

Our data on the inelastic scattering time $\tau_i(T)$ appear to be due to a combination of electron-electron and electron-phonon processes, as can be seen in Fig. 14, with the electron-phonon process dominating at high temperatures. We assume that the times can be summed according to

$$\tau_i^{-1}=\tau_{i,e\text{-}e}^{-1}+\tau_{i,e\text{-}p}^{-1} . \tag{21}$$

At low temperatures our data suggest that $\tau_i \propto T^{-1}$ and that electron-electron scattering is important. There have been two calculations of $\tau_{i,e\text{-}e}$: one by Abrahams *et al.*, for a disordered metal, and one by Altshuler *et al.* for electron-electron collisions with small energy transfer.[22,23] Both expressions are quite similar. Abraham *et al.* found that[22]

$$\tau_{i,e\text{-}e}=\tau_0\frac{E_F}{k_BT}\frac{1}{\ln(T_1/T)} , \tag{22}$$

where

$$T_1=\frac{\hbar}{k_B}D\epsilon^2\epsilon_0^2/e^4 . \tag{23}$$

Here, ϵ_0 is the permittivity constant (8.85×10^{-12} $C^2/N\,m^2$), $\tau_0=d/v_F$, and ϵ is a parameter defined in terms of the screening length l_s as

$$\epsilon=D\hbar/l_s^2 . \tag{24}$$

Thus we find for T_1 the expression

$$T_1=\frac{\hbar^3}{k_B}\frac{v_F^3d^3}{27}\frac{1}{l_s^4}\frac{\epsilon_0^2}{\epsilon^4} . \tag{25}$$

The Altshuler *et al.* expression for $\tau_{i,e\text{-}e}$ is[23]

$$\begin{aligned}\tau_{i,e\text{-}e}&=\frac{2}{k_BT}\frac{m_e}{3}v_Fd\frac{1}{\ln(v_Fdm_e/3\hbar)}\\&=\tfrac{4}{3}\tau_0\frac{E_F}{k_BT}\frac{1}{\ln(v_Fdm_e/3\hbar)} .\end{aligned} \tag{26}$$

There is one major difference between Eqs. (22) and (26) in that the argument of the Abraham ln term T_1/T is a factor of about 10^6 greater than the argument $v_Fdm_e/3\hbar$. As a result, the Altshuler expression yields weaker scattering times by a factor of 5 compared to the times from the Abraham expression. The times of the Abraham expression are in good agreement with our 2-K values; disagreement in the worst case is a factor of 6. The linear dependence of τ_i on film thickness d seems to be followed more or less. More low-temperature measurements are required below 2 K to confirm the $\tau_{i,e\text{-}e} \propto T^{-1}$ dependence.

A major problem appears above 10 K where the inelastic scattering times are much stronger (smaller in magnitude) than the times predicted by most theories; differences of factors of 10^2 to 10^5 are common. In fact, Bergmann was so concerned with the disagreement that he made independent measurements of the electron-phonon time in Au films and found that these values agreed within a factor of 2 with the inelastic times obtained from the MC data.[24] Thus, he concluded that the electron-phonon processes are an essential factor in the inelastic time.

We summarize and evaluate in the following some of the theoretical expressions of $\tau_{i,e\text{-}p}$ for the case of a 100-Å Cu film (these results should be compared to our experimental observation that $\tau_i=3.4\times10^{-10}/T^2$ above 10 K).

(a) Electron-electron scattering on the Fermi sphere near $T=0$ K:[25]

$$\tau_{i,e\text{-}e}=\frac{8}{\pi}\frac{\hbar E_F}{(k_BT)^2}\frac{1}{\left[1+\frac{4\sqrt{3}}{\pi}\left[\frac{1}{k_Fl_0}\right]^{3/2}\left[\frac{E_F}{k_BT}\right]^{1/2}\right]}\cong\frac{1.3\times10^{-6}}{T^2}\ , \tag{27}$$

where $E_F=7$ eV for Cu and $k_F=1.36\times10^8$ cm^{-1}.

(b) Electron-phonon interaction obtained from an impurity correction:[26]

$$\tau_{i,e\text{-}p}=\frac{\mathscr{L}}{n}Mm_e\frac{l_0}{\overline{(1/c^3)}}\frac{1}{(k_BT)^2}\frac{1}{2.47}\cong\frac{5.6\times10^{-7}}{T^2}\ , \tag{28}$$

where n is the electron density, $\mathscr{L}$ is the number of atoms per volume, M is the ion mass, m_e is the electron mass and $\overline{(1/c^3)}$ is an average over the sound velocities ($v_L=4700$ m/sec, $v_T=2100$ m/sec).

(c) According to Takayama, and electron-phonon interaction arising from electron diffusion in the field of the impurities leads to[27]

$$\tau_{i,e\text{-}p}=\frac{k_Fl_0}{2\pi^2\lambda}\frac{\hbar}{k_B\Theta_D}\left[\frac{\Theta_D}{T}\right]^2\cong\frac{1.6\times10^{-8}}{T^2}\ , \tag{29}$$

where $\Theta_D=315$ K for Cu and λ is a constant on the order of unity.

(d) Electron-phonon collisions in the presence of impurities:[28]

$$\tau_{i,e\text{-}p}=\frac{1}{\Lambda}\frac{\hbar^3\omega_1}{(k_BT)^3}\frac{1}{B(k_BT/\hbar\omega_1)}\cong\frac{1.5\times10^{-7}}{T^3}\ , \tag{30}$$

where

$$\omega_1=c_Lk_F,\quad \Lambda=\frac{Z\hbar^2\omega_1^2}{3m_eMc_L^4},\quad \eta=\frac{c_L}{c_T}\ . \tag{31}$$

Z is the number of free electrons per atom ($Z=1$ for Cu) and $B(k_BT/\hbar\omega_1)$ is determined from Fig. 8 of Ref. 28. From Fig. 8 at $T=10$ K, $B=30$. Interestingly, B increases as k_Fl_0 decreases, reaching a maximum value of 60 when $k_Fl_0=30$. Thus, B scales up with decreasing film thickness $d=l_0$.

The Schmid predictions of Eq. (30) are reasonable, being a factor of 10 too large compared to the observed τ_i times at high temperatures. But, when this prediction is used, together with the prediction of Abraham *et al.* of Eq. (22) in Eq. (21), to yield the total inelastic time τ_i, the agreement is good, as shown by the solid curve c in Fig. 14 for the 56-Å film. No adjustable parameters were used to obtain curve c. The agreement can be made better if we scale the Schmid expression smaller by a factor of 3, as indicated by curve d in Fig. 14; however, we have no theoretical justification for this scaling step. Thus, the "apparent" T^{-2} behavior of T_i at high temperatures appears to arise from the reciprocal summing of the T^{-1} and T^{-3} scattering mechanisms. Certainly, additional and more accurate MC measurements are needed above 20 K to confirm the $\tau_i\propto T^3$ dependence at the higher temperatures.

VII. CONCLUSIONS

We have presented resistance and MC data on clean thin Cu films. Values for the spin-orbit and inelastic scattering times derived from the data have been compared to theoretical predictions, and agreement between theory and experiment is generally good to within one order of magnitude or better. More theoretical work is needed on the problems of the electron-phonon elastic scattering and on the WL conductance prediction in low magnetic fields. In addition, electron-electron interaction effects gave an important contribution to the resistance at low temperature. Here, additional theoretical work is needed to verify the suggested $2(1-F)$ prefactor of the $\ln T$ electron-electron interaction contribution required to explain the data. And, from the experimental side, more low- and high-temperature MC data are required to better define the temperature dependence of the inelastic time at these temperatures.

ACKNOWLEDGMENTS

We are indebted to many people who helped us in many stages of this investigation. We extend our thanks to Jo'se Lereah for taking the TEM pictures, and we acknowledge the assistance of Yo'av Yigal in making the carbon substrates required for the TEM pictures. We are obliged to Professor Zvi Ovadyahu for thin high-purity Cu Slices used in the evaporation of our films. We thank Professor Ora Entin and Professor Joseph Imry for informative discussions. This work was partially supported by a grant from the family of Raymond and Beverly Sackler.

[1]D. J. Thouless, Phys. Rev. Lett. **39**, 1167 (1977).
[2]E. Abrahams, P. W. Anderson, D. C. Licciardello, and T. V. Ramakrishnan, Phys. Rev. Lett. **42**, 673 (1979).
[3]B. L. Altshuler, A. G. Aronov, and P. A. Lee, Phys. Rev. Lett. **44**, 1288 (1980).
[4]B. L. Altshuler, D. Khmel'nitskii, A. I. Larkin, and P. Lee, Phys. Rev. B **22**, 5142 (1980).
[5]H. Fukuyama, J. Phys. Soc. Jpn. **48**, 2169 (1980).
[6]B. L. Altshuler, A. G. Aronov, and D. Khmel'nitskii, Solid State Commun. **39**, 619 (1981).
[7]Yu. F. Komnik, E. I. Bukhshtab, A. V. Butenko, and V. V. Andrievsky, Solid State Commun. **44**, 865 (1982).
[8]L. Van den Dries, C. Van Haesendonck, Y. Bruynseraede, and G. Deutscher, Phys. Rev. Lett. **46**, 565 (1981); C. Van Haesendonck, L. Van den Dries, Y. Bruynseraede, and G. Deutscher, Phys. Rev. B **25**, 5090 (1982).
[9]M. E. Gershenson and V. N. Gubankov, Pis'ma Zh. Eksp. Teor. Fiz. **34**, 30 (1981) [JETP Lett. **34**, 32 (1981)]; M. E. Gershenson and V. N. Gubankov, Solid State Commun. **41**, 33 (1982); M. E. Gershenson, B. N. Gubankov, and Yu. Zhuravlev, Zh. Eksp. Teor. Fiz. **83**, 2348 (1982) [Sov. Phys.—JETP **56**, 1362 (1982)].

[10](a) D. Abraham and R. Rosenbaum, Phys. Rev. B **27**, 1409 (1982); (b) **27**, 1413 (1982); (c) J. Phys. C **17**, 2627 (1984); (d) R. Rosenbaum, Phys. Rev. B **32**, 2190 (1985).
[11]A. E. White, M. Tinkham, W. J. Skocpol, and D. C. Flanders, Phys. Rev. Lett. **48**, 1752 (1982).
[12]R. Meservey and P. M. Tedrow, Phys. Rev. Lett. **41**, 805 (1978).
[13]S. Hikami, A. Larkin, and Y. Nagaoka, Prog. Theor. Phys. **63**, 707 (1980).
[14]G. Bergmann, Phys. Rev. Lett. **48**, 1046 (1982).
[15]G. Bergmann, Phys. Rev. Lett. **49**, 162 (1982).
[16]S. Maekawa and H. Fukuyama, J. Phys. Soc. Jpn. **50**, 2516 (1981).
[17]H. Fukuyama, J. Phys. Soc. Jpn. **50**, 3407 (1981); **51**, 1105 (1982).
[18]P. A. Lee and T. V. Ramakrishnan, Phys. Rev. B **26**, 4009 (1982).
[19]N. W. Ashcroft and N. D. Mermin, *Solid State Physics* (Holt Rinehart and Winston, New York, 1976), pp. 34 and 342.
[20]A. Palevski and G. Deutscher (unpublished).
[21]A. Palevski and G. Deutscher, J. Phys. A **17**, L895 (1984).
[22]E. Abrahams, P. W. Anderson, P. A. Lee, and T. V. Ramakrishnan, Phys. Rev. **24**, 6783 (1981).
[23]Bv. L. Altshuler, A. G. Aronov, and D. E. Khmelnitsky, Solid State Phys. C **15**, 7367 (1982).
[24]G. Bergmann, Solid State Commun. **46**, 347 (1983).
[25]A. Schmid, Z. Phys. **271**, 251 (1974).
[26]G. Bergmann, Z. Phys. B **48**, 5 (1982).
[27]H. Takayama, Z. Phys. **263**, 329 (1973).
[28]A. Schmid, in *Localization, Interaction, and Transport Phenomena,* Proceedings of the International Conference, edited by B. Kramer, G. Bergmann, and Y. Bruynseraede (Springer-Verlag, New York, 1984), p. 212.

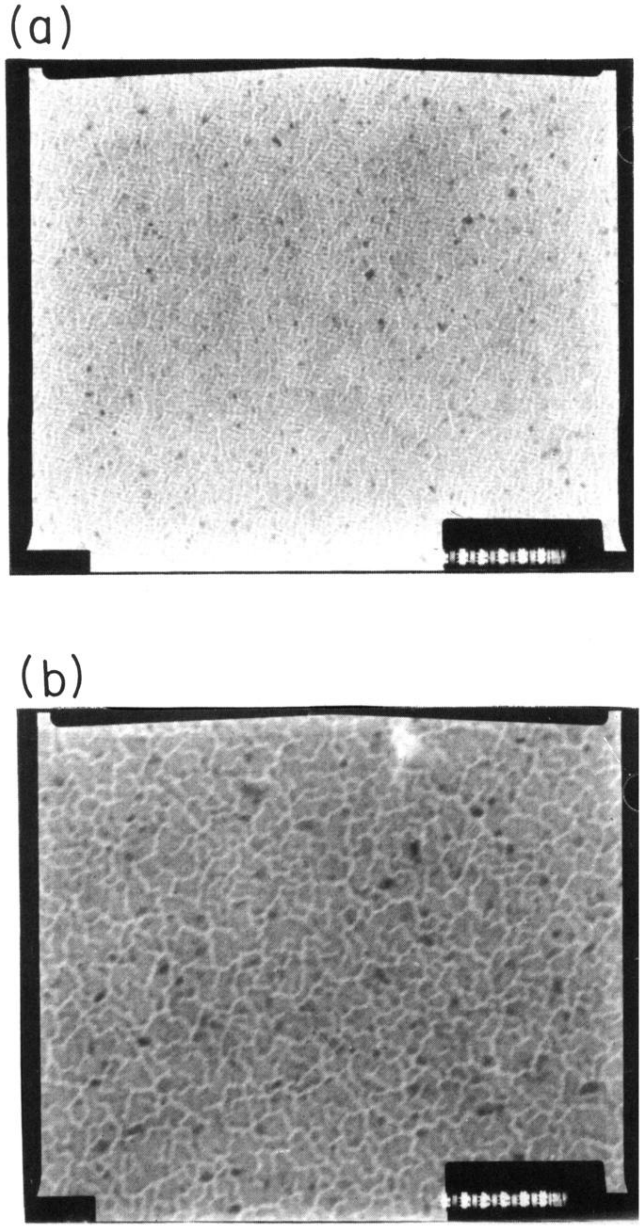

FIG. 2. TEM pictures of a 60-A Cu film: (a) unoxidized semicontinuous film showing the weak appearance of cracks, and (b) oxidized noncontinuous film showing isolated 75-Å islands separated by cracks permeating throughout the entire film.